LAWRENCE
LIVERMORE
NATIONAL
LABORATORY

Simulation Study of Near-Surface Coupling of Nuclear Devices vs. Equivalent High-Explosive Charges

K. B. Fournier, O. R. Walton, R. Benjamin, W. H. Dunlop

October 8, 2014

Disclaimer

This document was prepared as an account of work sponsored by an agency of the United States government. Neither the United States government nor Lawrence Livermore National Security, LLC, nor any of their employees makes any warranty, expressed or implied, or assumes any legal liability or responsibility for the accuracy, completeness, or usefulness of any information, apparatus, product, or process disclosed, or represents that its use would not infringe privately owned rights. Reference herein to any specific commercial product, process, or service by trade name, trademark, manufacturer, or otherwise does not necessarily constitute or imply its endorsement, recommendation, or favoring by the United States government or Lawrence Livermore National Security, LLC. The views and opinions of authors expressed herein do not necessarily state or reflect those of the United States government or Lawrence Livermore National Security, LLC, and shall not be used for advertising or product endorsement purposes.

Simulation Study of Near-Surface Coupling of

Nuclear Devices vs. Equivalent High-Explosive Charges

Kevin Fournier, Otis Walton, Russ Benjamin, William Dunlop

ABSTRACT

A computational study was performed to examine the differences in near-surface ground-waves and air-blast waves generated by high-explosive energy sources and those generated by much higher energy-density low-yield nuclear sources. The study examined the effect of explosive-source emplacement (i.e., height-of-burst, HOB, or depth-of-burial, DOB) over a range from depths of -35m to heights of 20m, for explosions with an explosive yield of 1-kt. The chemical explosive was modeled by a JWL equation-of-state model for a ~14m diameter sphere of ANFO (~1,200,000kg – 1 kt equivalent yield), and the high-energy-density source was modeled as a one tonne (1000 kg) plasma of 'Iron-gas' (utilizing LLNL's tabular equation-of-state database, LEOS) in a 2m diameter sphere, with a total internal-energy content equivalent to 1 kt.

A consistent equivalent-yield coupling-factor approach was developed to compare the behavior of the two sources. The results indicate that the equivalent-yield coupling-factor for air-blasts from 1 kt ANFO explosions varies monotonically and continuously from a nearly perfect reflected wave off of the ground surface for a HOB≈20m, to a coupling factor of nearly zero at DOB≈-25m. The nuclear air-blast coupling curve, on the other hand, remained nearly equal to a perfectly reflected wave all the way down to HOB's very near zero, and then quickly dropped to a value near zero for explosions with a DOB≈-10m. The near-surface ground-wave traveling horizontally out from the explosive source region to distances of 100's of meters exhibited equivalent-yield coupling-factors that varied nearly linearly with HOB/DOB for the simulated ANFO explosive source, going from a value near zero at HOB≈5m to nearly one at DOB≈-25m. The nuclear-source generated near-surface ground wave coupling-factor remained near zero for almost all HOB's greater than zero, and then appeared to vary nearly-linearly with depth-of-burial until it reached a value of one at a DOB between 15m and 20m. These simulations confirm the expected result that the variation of coupling to the ground, or the air, changes much more rapidly with emplacement location for a high-energy-density (i.e., nuclear-like) explosive source than it does for relatively low-energy-density chemical explosive sources.

The Energy Partitioning, Energy Coupling (EPEC) platform at LLNL utilizes laser energy from one quad (i.e. 4-laser beams) of the 192-beam NIF Laser bank to deliver ~10kJ of energy to 1mg of silver in a hohlraum creating an effective small-explosive 'source' with an energy density comparable to those in low-yield nuclear devices. Such experiments have the potential to provide direct experimental confirmation of the simulation results obtained in this study, at a physical scale (and time-scale) which is a factor of 1000 smaller than the spatial- or temporal-scales typically encountered when dealing with nuclear explosions.

PRIOR WORK

In February 2013, we completed a proof-of-principle series of experiments at the National Ignition Facility (NIF) that demonstrated that one could simultaneously measure the arrival time and peak pressure of air blasts and the stress and pressures due to ground shock created by a high-energy-density explosion of comparable energy density to that of

a low-yield nuclear weapon. These proof-of-principal experiments were conducted using the Energy Partitioning, Energy Coupling (EPEC) platform.[1] Additionally, we demonstrated in those experiments that the x rays produced by the laser-driven target produced a fireball from which we could measure the history of the optical power emitted by the fireball and its interaction with the material perturbation caused by the expanding blast waves in our test atmosphere. These experiments were able to be carried out at energy densities characteristic of low-yield nuclear weapons using the capability of the NIF laser to focus one quad of laser beams with 10 kilojoules of energy into a spot only a few hundred microns in diameter in a billionth of a second. These proof-of-principle experiments demonstrated that changing the height of burst (HOB) of the energy source by a factor of ten (from 10 scaled meters to 1 scaled meter HOB) enhanced the ground coupling to the ground surrogate by a similar factor. Simultaneously, we saw that air-blast coupling diminished, although at this moment we are still determining a quantitative factor. [2]

Similarly, the state-of-the-art in energy partitioning, energy coupling studies that support the tools and techniques for prompt yield determination in support of an improvised nuclear device being detonated in an unknown emplacement has been advanced by recent chemical-explosive tests carried out under the auspices of the Defense Threat Reduction Agency. Detailed mapping of the ground shock and air-blast partitioning of the energy for scaled heights of burst has been accomplished.[3] However, those tests were not carried out with sources that had the energy densities of nuclear devices, nor were there any x rays present in the output of the high-explosive tests. As the next step in this research line, we have conducted a computational study comparing the partitioning of energy and coupling of effects for 1 kt nuclear devices and 1 kt high explosive blasts between 20 meters scaled height of burst and 30 meter scaled depth of burial.

In this study, to simplify the computational complexity, we have chosen to assume that the nuclear source is a primitive type of nuclear weapon that has significant surrounding material that absorbs the x ray flux leaving the device and reradiates it as thermal energy. Thus, for this study, this assumption simplifies the complexity of the calculations, but will have little effect on the comparison between the nuclear source and the high explosive source.

PROPOSED WORK AND SCIENTIFIC BASIS

We have demonstrated the ability to simulate nuclear weapon effects in laser-driven experiments at the NIF.[2] We have shown in the EPEC experiment that we can measure air-blast phenomena (arrival times, peak pressures), ground-shock phenomena (stresses and pressures) and optical histories of plasma fireballs. The EPEC system (Figure 1) is a pressure vessel that contains an atmosphere, a solid material that is a ground surrogate, a laser target that is an "energy pill" driving blast phenomena, and sensors to measure air pressure, ground shock and light emitted from the interaction of the target and the atmosphere. The EPEC laser-driven platform is unique in that through focusing of the laser energy of a single quad of NIF beams, the laser target in the experiment becomes a high-temperature plasma with energy density and energy per unit mass similar to a first-

generation nuclear device with a yield of approximately 2.5 kt. Through hydrodynamic scaling[4] the absolute values of pressures and shock-propagation velocities in the EPEC system are identical to those that would be obtained from the detonation of a 2.5 kt nuclear device at times and distances 1000 times greater than the times and distances at which measurements in the EPEC system are made. This is a critical point to emphasize since the partitioning of the energy in blast and shock phenomena between the ground and atmosphere is not well understood for explosions within a few tens of meters above the surface and is poorly understood for detonations slightly below the Earth's surface. It is only through the high energy density achieved in a laser experiment that, for simulated yields in the kt range, variation of the partitioning can be studied for scaled heights of burst (HOBs) less than 10 meters/kt$^{1/3}$ (see Figure 2). The physical scale of a high-explosive (HE) driven system in this yield range would be of the same order as the range of HOBs to be studied. As we will show in our calculations, the physical size of the HE driven system affects the results obtained in this near-surface regime. Therefore, NIF presently offers a unique ability to probe the physics of low-yield, near-surface nuclear detonations, in a way that cannot be studied via HE tests.
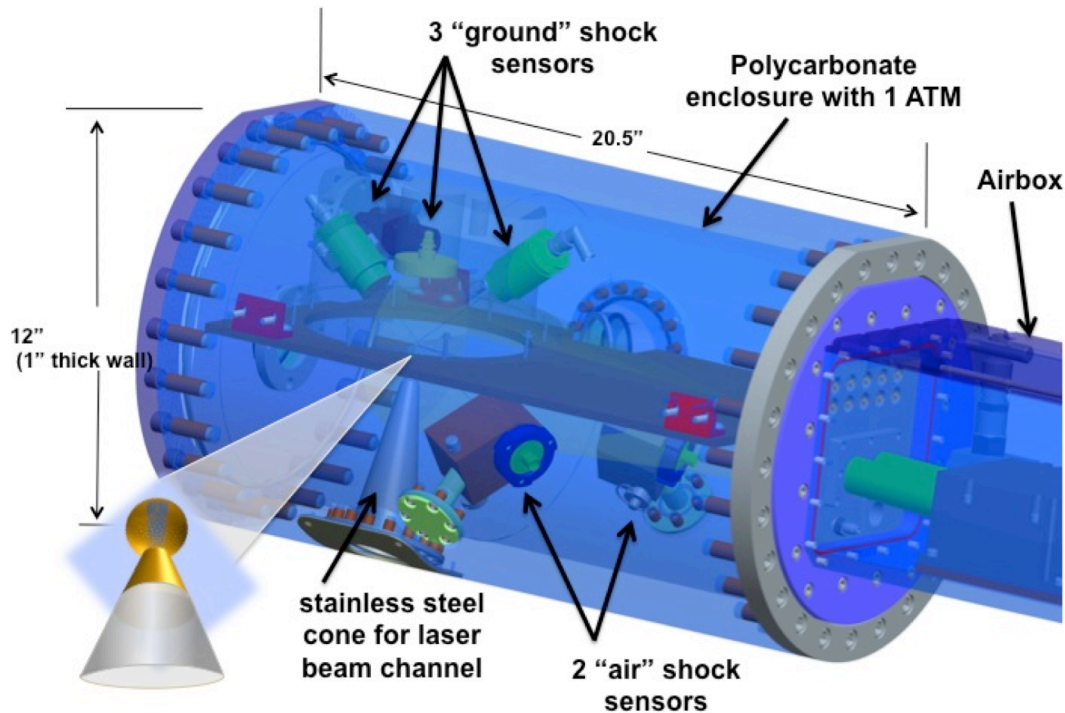

Figure 1. The integrated assembly for the Energy-Partitioning Energy-Coupling (EPEC) experiment shows ground-shock sensors embedded in the Earth-simulant, air-blast sensors, and a view of the 2-mm-diameter halfraum that is the target of the laser beams.

3

In the present study we have conducted a series of calculations to map out air blast and ground shock coupling at several heights of burst comparing high-explosive driven events to nuclear-explosive driven events. By definition 1 kiloton of TNT weighs 1000 tons, but many high explosive experiments are conducted with ANFO, which has a relative-effectiveness of about 0.82 of that of TNT meaning that about 1.22 kilotons of ANFO has the explosive energy of 1 kiloton of TNT. Additionally ANFO is usually handled as prill or granular solid with a bulk density of ~0.82g/cc, compared to a density of 1.6g/cc for TNT. Thus, the volume of ANFO required to produce a detonation of 1 kiloton of TNT equivalent is roughly twice as large as 1 kiloton of TNT. For a spherical charge of 1-kiloton explosive yield the diameter of an ANFO charge would be about one third larger than for TNT (e.g., ~7m radius for ANFO vs. ~5.3m radius for TNT). We chose to do all the high explosive calculations using ANFO as the source since this is the typical explosive charge used in current experimental studies with yields greater than 1-ton TNT equivalent.
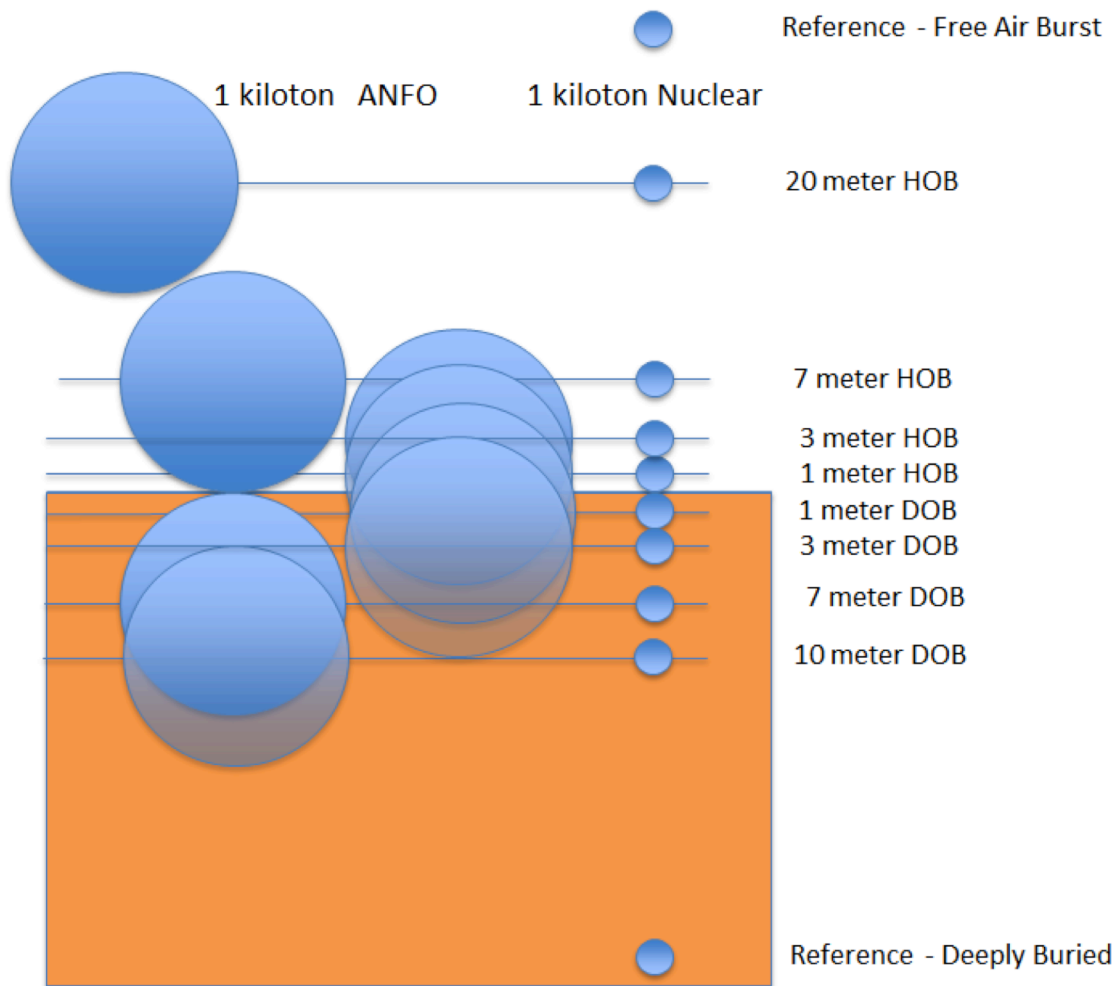
Figure 2. This figure shows the heights of burst and depths of burial proposed for the computational study. The circles represent the size of the explosive charge (ANFO– large circles and nuclear – small circles).

4

Figure 2 shows the set of calculations that were proposed to provide insight into the different effects that occur due to source-size issues. This set of calculations would also provide information useful in follow-on experiments in the EPEC platform. Specifically, we planned to examine the effects on the nuclear-driven air-blast and ground shock phenomena that result from contact/interaction with the ground surface and provide data that would help to quantify the air-blast and ground sensor responses to these effects. The resulting laser experiments that emulate a selected subset of configurations was chosen to span the range of HOB/DOB needed for this computational study.

We initially proposed a computational series to map out the coupling of energy to the air and ground at eight HOBs that ranged from 20 meter to -10 meters (negative heights of burst = depth of burial or DOB) as shown in Figure 2. The exact HOBs and DOBs for the study were adjusted during the computational campaign to fully cover the range of HOBs and DOBs needed, and in consideration of the difficulty of completing some of the calculations. The set of calculations performed and used to simulate HOBs and DOBs spanned the range from depths of -35m to heights of 20m, and also included free-air and deeply buried cases for comparison.

Reference calculations of a free-air burst and a deeply buried emplacement were included to establish baseline values for determining equivalent coupling factors for air blast and ground shock in the near surface cases. The deepest burial of the explosions in the computational parameter study was a fully buried energy source at -35 meters.

The yield in both the nuclear and chemical HE source calculations was chosen to be 1 kiloton (kt), which makes for easy scaled comparisons with historical data taken at other yields. For the nuclear case, the energy pill is quite small (a 2 m diameter source for each calculation). The ionizing-radiation components of the weapon output are completely absorbed within millimeters of the surface of the "device", i.e., completely within the ground medium for all buried devices with the exception of the 1 m depth of burial. For all the cases we used the purely hydrodynamics geophysical code GEODYN[4,5,6] to model shock and cratering phenomena. In the case of the 35 m DOB, the chemical explosive is completely under the surface of the Earth whether it is modeled as TNT (~5.3 m radius) or ANFO (~7 m radius). Since the upper extent of the chemical HE charge is 28 meters from the ground surface for the case of a 1 kt ANFO charge, it is expected to result in interactions between the blast energy and the ground and air similar to the case of the 30-m-buried nuclear device.

While it is recognized that different strength ground-shocks and different crater sizes will result from the same explosive charges in different geologic materials, this study focused on one representative material for which good material models exist (e.g. dry Indiana limestone with modest porosity was chosen as a representative geologic material). The aim of the study is to determine differences between near-surface HE and nuclear explosions. Similar differences would be expected with other geologic materials, and determination of the effects of geotechnical material properties on near-surface-burst coupling may be the subject of future studies. For example, the limestone model used in these simulations is a reasonably competent rock with an unconfined strength of approximately 75 MPa. It is expected that a weaker alluvial material would require deeper burial before there would be no breakout of the blast wave to the air. For near-

surface bursts a weaker material would have greater mass ejected from the crater, which might affect the magnitude of resulting air-blasts. Future simulations could assist in establishing the magnitude of such effects.

The upper range of the height of burst for our proposed computational parameter study was the 20 m HOB case. For a 1 kt yield, there may be "contact burst" phenomena in the observed air-blast effects where the blast wave from the explosion will interact with the ground, and reflections from the ground will modify the propagation of the blast wave. For this study our choice of a low efficiency device, i.e. high mass per yield, eliminates the need to account for the x-ray flux emanating from the nuclear source. A follow-on study could look at the differences between high mass and low mass nuclear devices. This would require using the code RAPTOR to transport source x-ray radiation through the atmosphere for these nuclear cases. The result of such a study would be an understanding of the temperatures induced within approximately 20 meters in air due to x-ray preheat. This pre-heated air can strongly affect the propagation of the subsequent blast wave that propagates from the burst point. Also this additional study could look at the deposition of x-ray energy on the ground directly under the detonation point. For buried explosions, past numerical studies have shown little difference between hydro-only and coupled radiation-hydrodynamic representations of the early expanding ionized gas representing a nuclear explosion.

Even for these low efficiency devices the sound-speed in the shock-heated fireball is still extremely high (on the order of 10's of km/s) so it is still a reasonable representation of a high energy density nuclear explosion; but it represents a lower limit of the possible nuclear sources.

THE GEODYN CODE:

The hydrodynamic code GEODYN[4-6] was developed at LLNL and incorporates physical models to describe fully a broad range of phenomena including shock and thermodynamic behavior. GEODYN is an Eulerian code, which means the mesh or background is stationary and the material is allowed to move though stationary cells, with adaptive mesh refinement (AMR)[6]. The adaptive mesh means that the code has the ability to vary the level of detail of the background. An Eulerian code with AMR such as GEODYN allows for rigorous high numerical resolution in areas in one part of a problem and lower resolution in less sensitive areas.

A common practice in performing computational studies of the effects of nuclear explosions is to run hydrodynamics-only simulations with the 'energetic source' represented as an expanding plasma of vaporized/ionized metal (usually approximated as a sphere of uniformly heated 'iron-gas') into which the released nuclear explosion energy is assumed to be distributed as an 'initial-state' of thermal energy for the molecules/ions. Such simplified simulations ignore radiation and thermal transport effects during the expansion of the simulated plasma/vapor. They are computationally relatively fast running, and capture the majority of the effects of the expanding shock wave in the surrounding ground and/or air (with the largest errors assumed to be within the fireball, for explosions in air, where radiation transport can play a significant role). For buried

explosions the calculated outgoing shock behavior in such simulations is generally within a few percent of comparable values obtained using simulations with full radiation/hydrodynamic effects included (e.g., for outgoing shock-wave parameters such as peak-pressure, arrival-time, and impulse in the first positive pressure pulse). The near-field air-blast fireball behavior is less well represented by such simulations, but far from the fireball region, the air blast results from hydro-only simulations are reasonably similar to simulations that include thermal/radiation effects.

THE CALCULATIONS:

Configurations at a dozen different heights-of-burst/depths-of-burial plus one free-air and one deeply buried case were simulated using an ANFO energy source. Configurations at 7 different heights-of-burst/depths-of-burial plus free-air and deeply buried cases were simulated using an iron-gas high-energy-density source (representing a nuclear explosion energy source). Additional nuclear cases are running, but at the time of preparation of this report had not run far enough to provide useful late-time ground shock or air-blast wave information. The turbulence in the nuclear energy density calculations near the surface was extreme, resulting in multiple-levels of adaptive mesh refinement, attempting to resolve interfaces between materials, along with mixed-material cells, high temperatures and high sound-speeds – causing some numerical difficulties resolving strength models for 'blended' materials. Images of the early-time pressure and velocity waves from a representative set of the calculations are included below (Figures 3-8) in order to provide at least a sense of what is occurring in the computations. Our analysis is taken from the calculations shown in Figure 2, plus a few additional configurations at greater depths, run as it became apparent that the coupling curves were not near their asymptotic values at a depth of only 10m.

It is clear from Figure 2 that until the ANFO charges are buried at least 7 meters there is no/little overburden over the ANFO explosions, whereas at a depth of 7 meters there is a 6-meter overburden above the nuclear charges. At depths of burial more than 20 meters the overburdens are not substantially different between the ANFO charge and the nuclear charge. Thus, we expect that, at DOBs ≥ 20m, the calculated shock fronts from these simulations would start to approach the traditional ratio of 2 times greater effectiveness in ground coupling for deeply-buried chemical explosions vs deeply-buried nuclear explosions.

Blast waves from simulated free-air nuclear (i.e., high-energy density) sources and chemical explosions are described in detail in the text by Kinney & Graham [K&G][7] and Glasstone & Dolan [G&D][8]. They show that the air-blast from nuclear sources tends to be narrower than the air-blast wave from chemical explosions, and at very short distances from the explosion, the nuclear blast wave exhibits higher peak pressure than the chemical explosion. Over most of the scaled ranges of interest for studying blast waves, they find that the air-blast peak-pressures from chemical explosions exceeds those from nuclear sources; however, at very long distances the differences decrease in magnitude. K&G describe reflections from the ground surface for near-surface air blasts resulting in a doubling of the effective source energy, and resulting shock parameters. Both the K&G text and historical data from nuclear tests (as well as past simulations) show that a Mach-

stem effect occurs for low elevation nuclear bursts. This effect is created when the reflected wave off of the ground travels through shock-heated air, which has a much higher sound speed than unshocked air. The resultant combined outgoing and reflected wave has a stronger outgoing horizontal air-blast near the ground surface, the effect of which tends to peak at scaled heights of burst around 200m/kt$^{1/3}$. At the highest height of burst in this series of simulations (20 meters) Mach-stem effects (As observed in Figure 3) have a minimal effect at surface ranges beyond 200m, so that at elevations less than 20m we generally expected both the chemical and the nuclear explosions to exhibit near-ground-surface air-blast waves, at distances of a few hundred meters, that are nearly equal to the free-air blast wave from a similar explosion with twice the actual yield (i.e., a nearly perfect reflection of the air-blast from the ground surface).

The following figures (3 – 8) are comparisons of the calculations of the early time evolution of the explosions of the nuclear device (on the left in each figure) and the high explosive charge (on the right in each figure). These comparisons are presented for a representative set of the heights of burst and depths of burial in the computational study. While these provide a sense of the differences in the evolution of the shock and blast waves, the detailed analysis of the calculated strength of the shock waves is presented in sections of this report following the figures from the calculations.

These figures show, in the first row of pictures, the initial configuration for each simulation as a density plot, demonstrating the physical differences between the starting conditions for the simulations. The second and third rows of pictures show the pressure (left half) and the velocity (right half) for these explosions at 5 ms (second row) and 20 ms (third row). These early time pictures were chosen to demonstrate that these two near-surface systems evolve differently as a function of time. The color scales for the pressure and velocity fields at each time are the same allowing one to contrast these parameters for the nuclear and HE cases.

Note that for both the air blasts and shallowly buried targets (DOB < 10m), the physical extent of the nuclear explosion is larger than the HE explosion at these early times. This is due to the non-linear response of the air to the high temperatures in the nuclear explosion. This allows the nuclear explosion to expand rapidly while the HE is burning. Once the explosives are buried, this effect disappears because the non-linear response of the air doesn't exist in the ground and, after the HE has burned, the two explosions are much closer in size.

Note also that at any given time in both the air blasts and shallowly buried emplacement (DOB < 5m), the HE explosions exhibit higher pressures and velocities than the nuclear explosions. This is largely due to the smaller extent of the HE explosion (from an air blast or shallowly buried emplacement) resulting in a higher average energy density, over the region shocked by the outgoing wave at a given time, an effect that largely disappears when the explosions are effectively fully buried (DOB ≥ 20m) and are more nearly the same size at the same time (See Figure 8). We believe if the air blast and shallowly buried explosions were plotted against each other at the same size rather than at the same time, this effect would disappear.
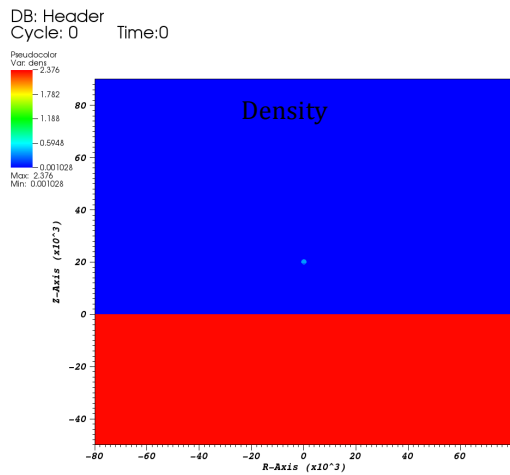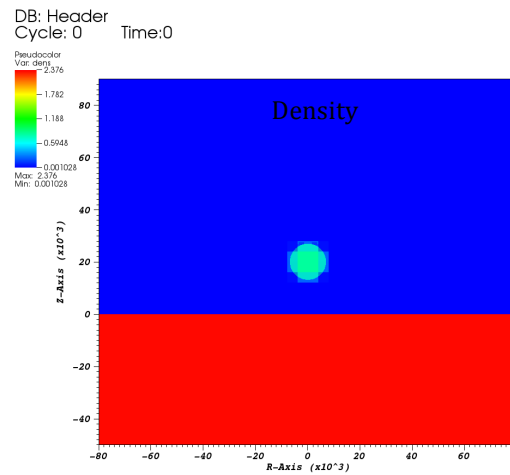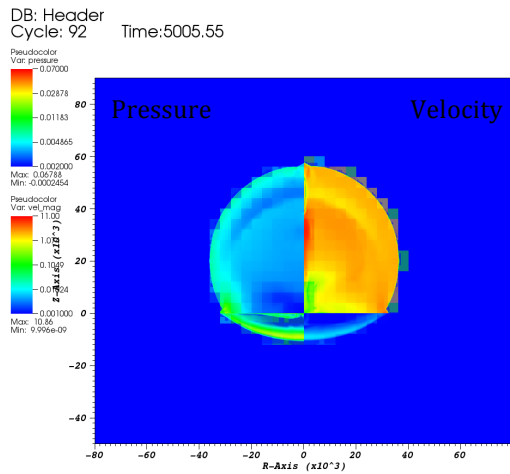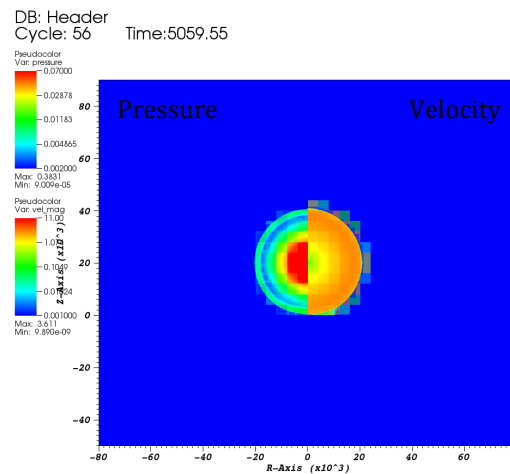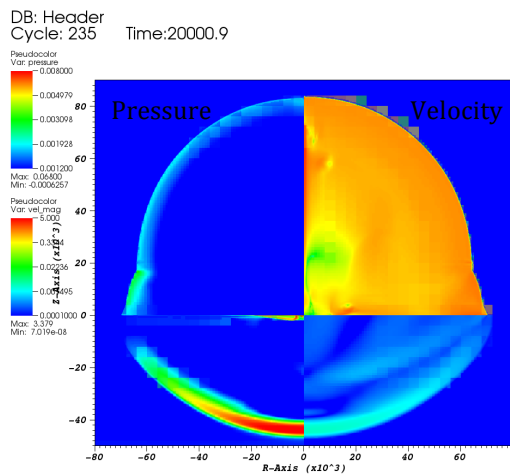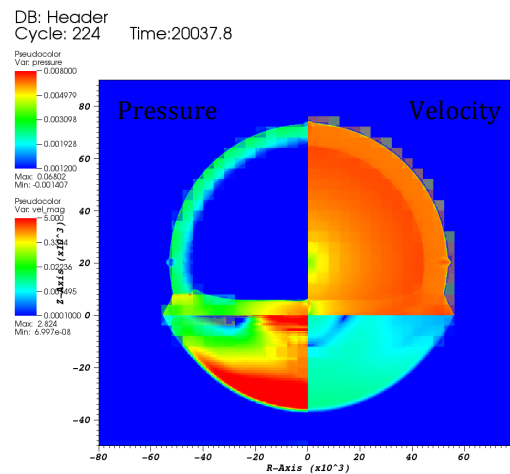
Figure 3. Comparison of the early time behavior of the nuclear (left) and HE explosions (right) for an HOB of 20m.

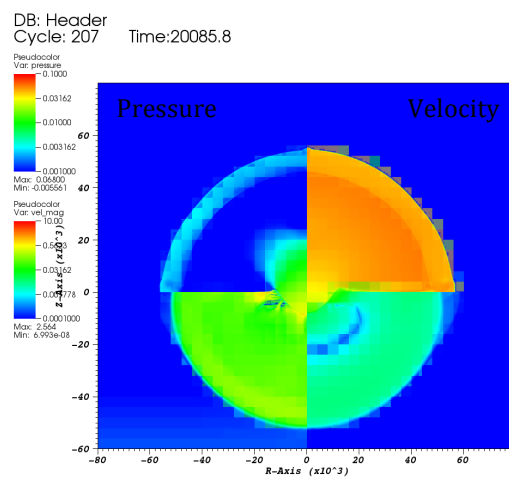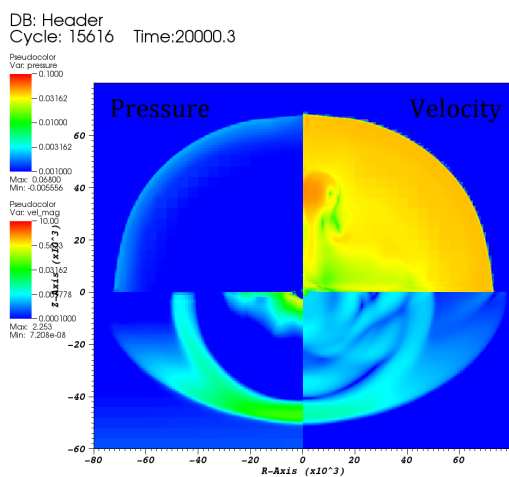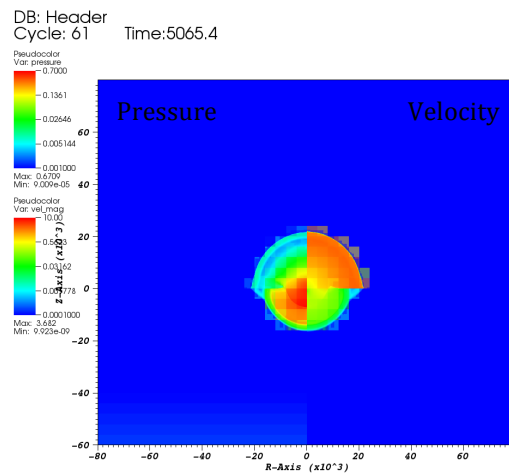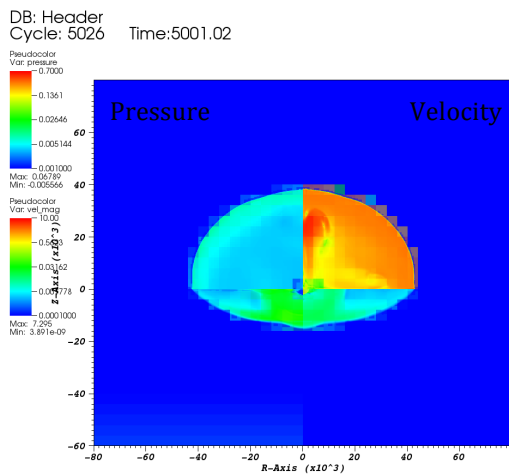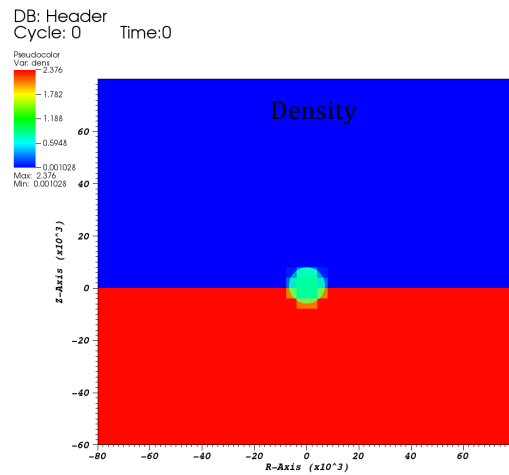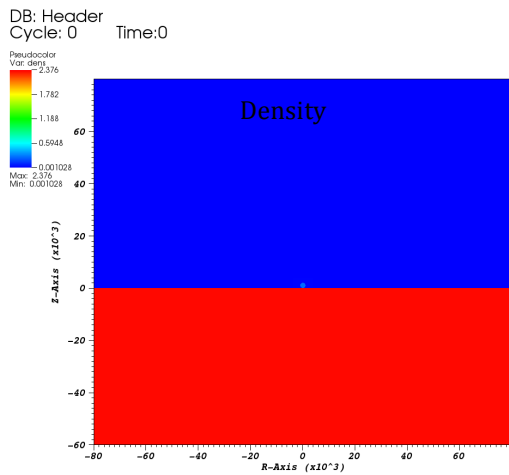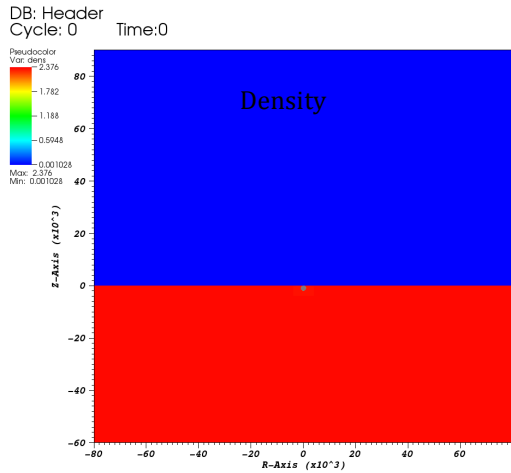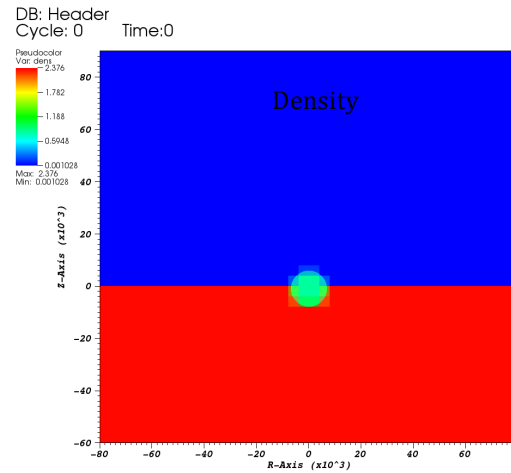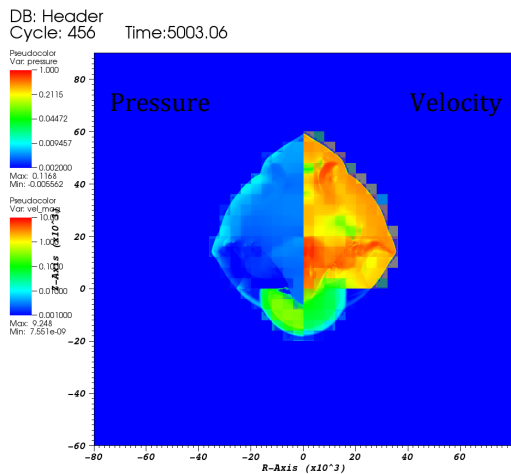**Figure 4.** Comparison of the early time behavior of the nuclear (left) and HE explosions (right) for an HOB of 1m.

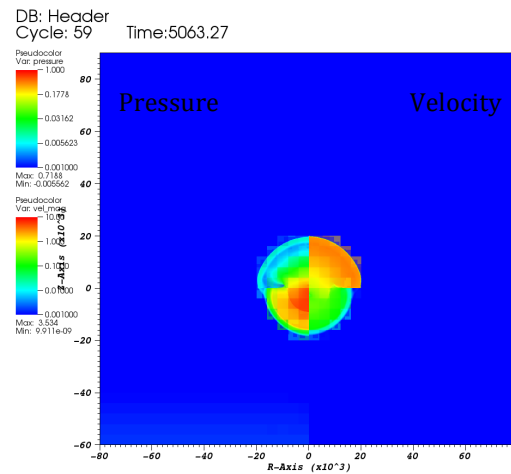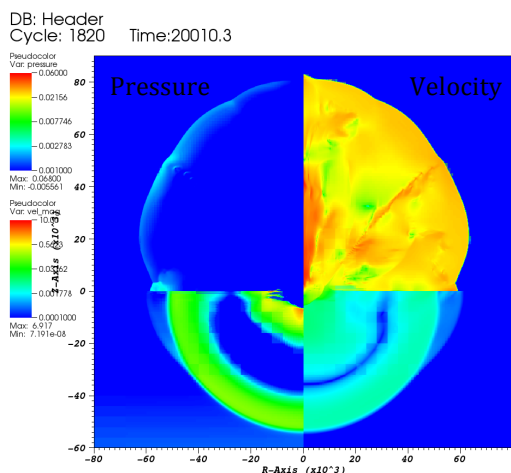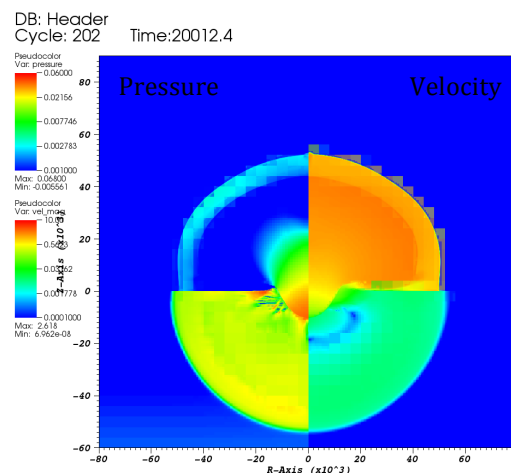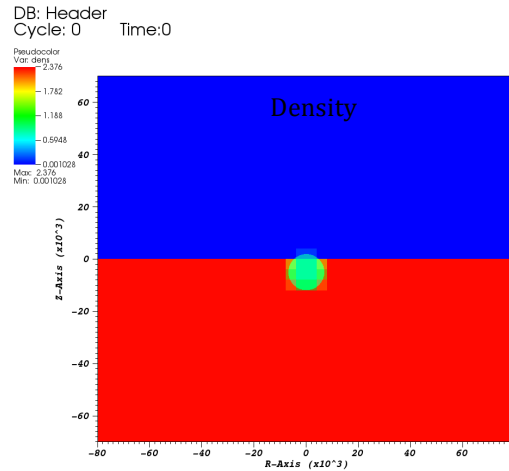**Figure 5**. Comparison of the early time behavior of the nuclear (left) and HE explosions (right) for a DOB of 1m.
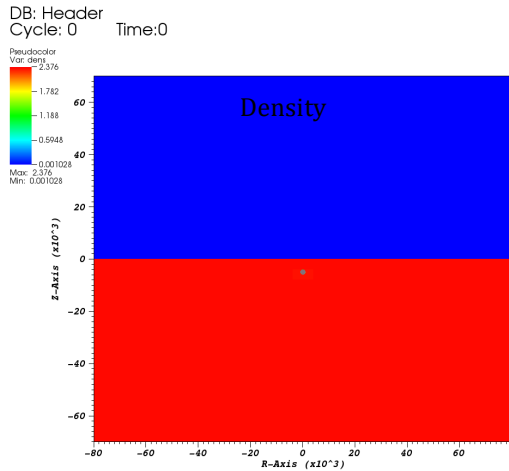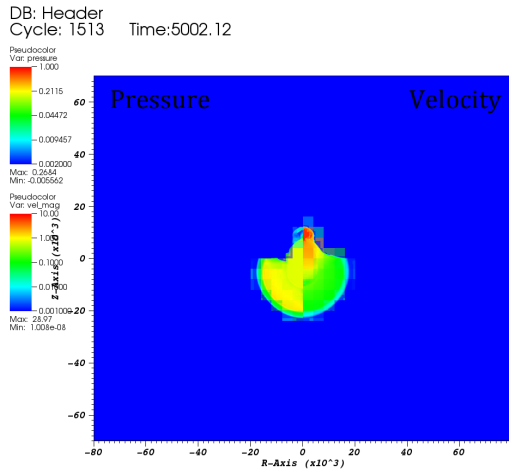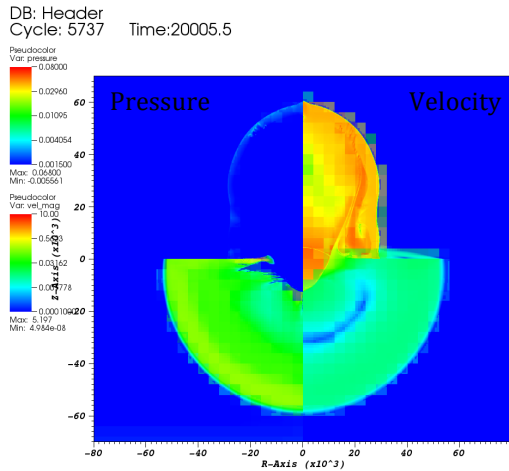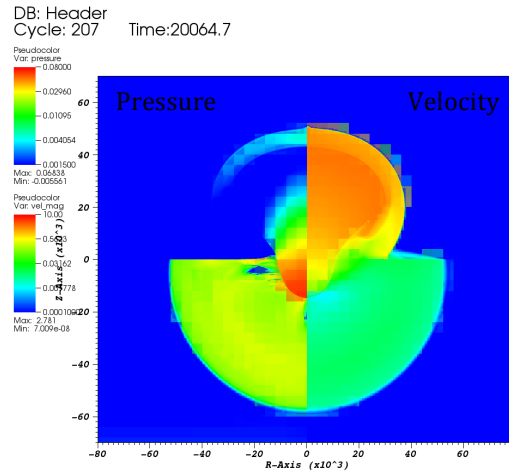
Figure 6. Comparison of the early time behavior of the nuclear (left) and HE explosions (right) for a DOB of 5m.
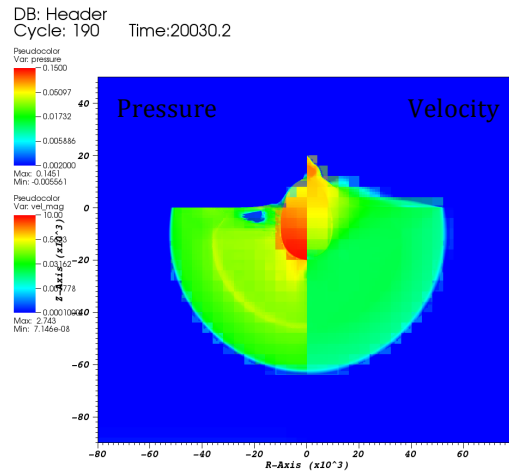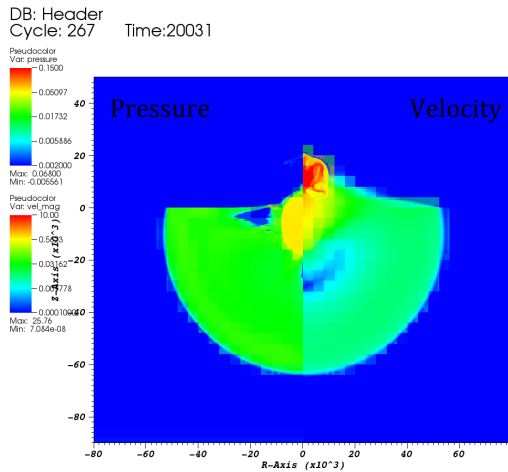
Figure 7. Comparison of the early time behavior of the nuclear (left) and HE explosions (right) for a DOB of 10m.

13
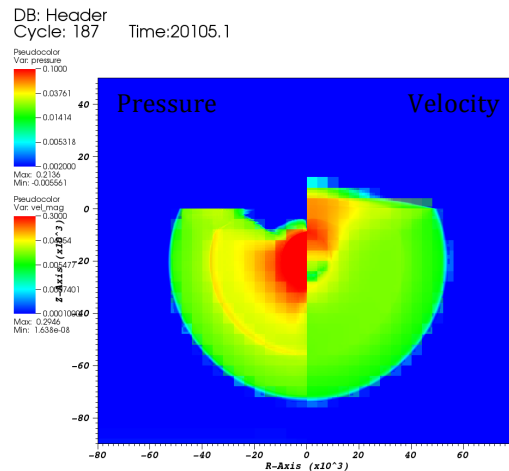
Figure 8. Comparison of the early time behavior of the nuclear (left) and HE explosions (right) for a DOB of 20m.

14

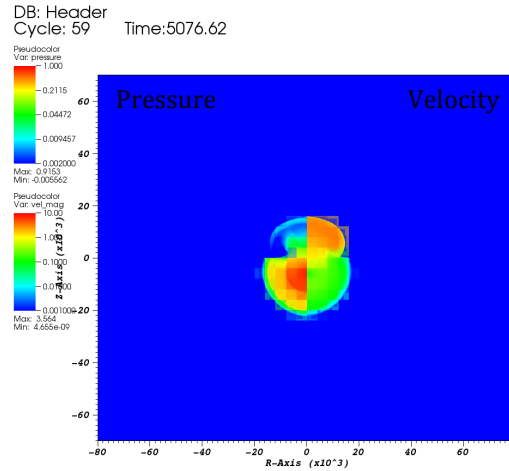Analysis of the pictures obtained during the simulations of each configuration, both high explosive and nuclear cases, show qualitatively the differences between 1 kt of high explosive and 1 kt of nuclear equivalent for each of the HOB / DOB in the ensemble of calculations. While this gives a sense of the differences between the calculations with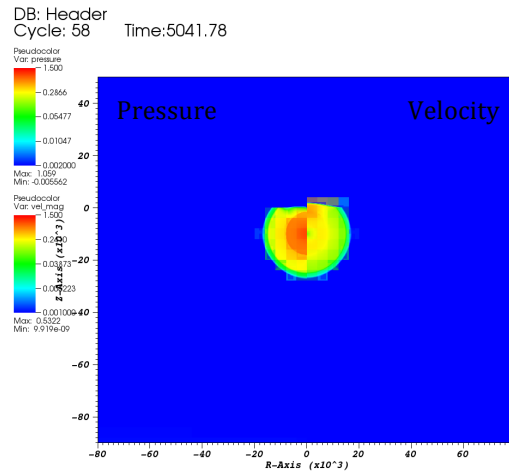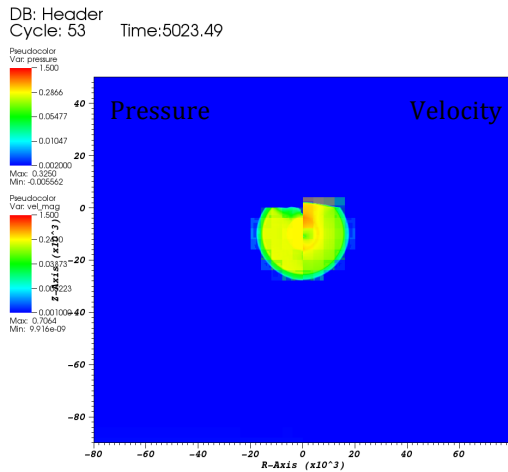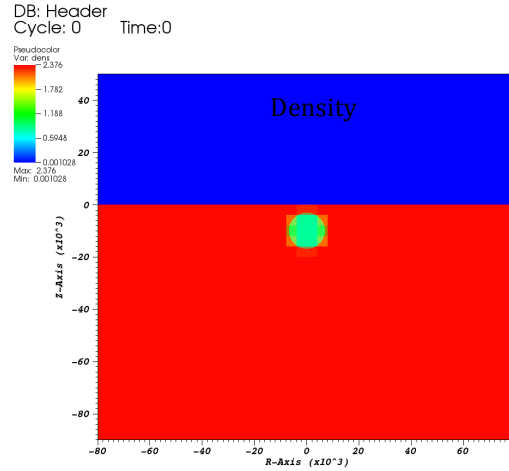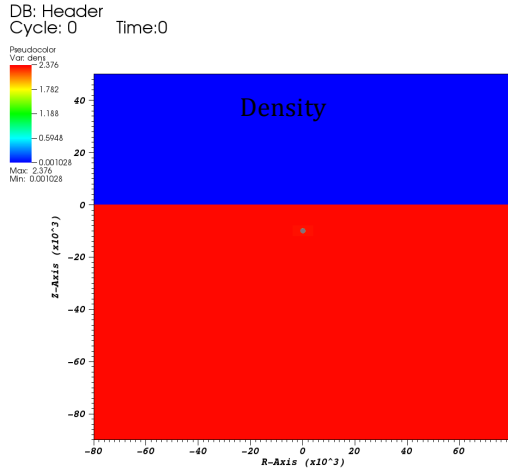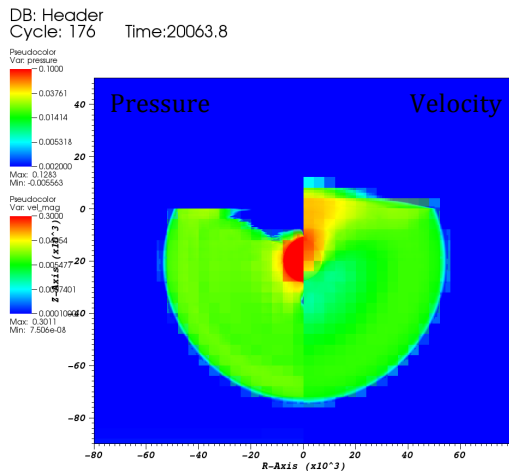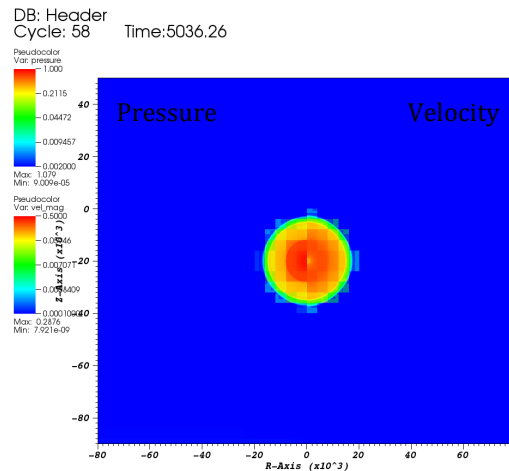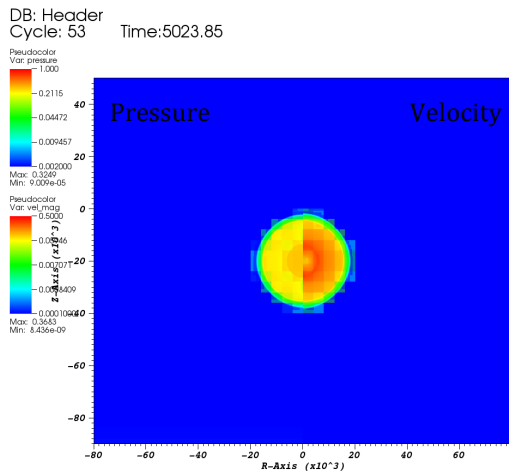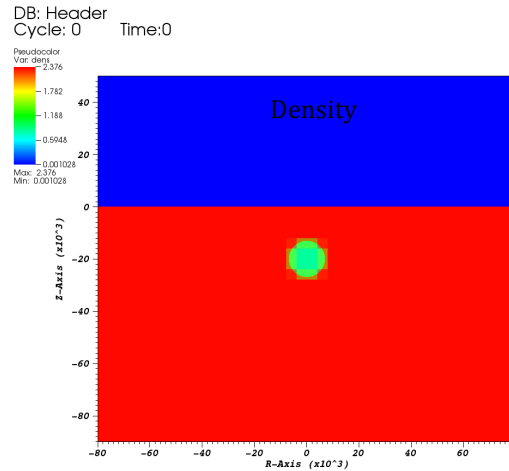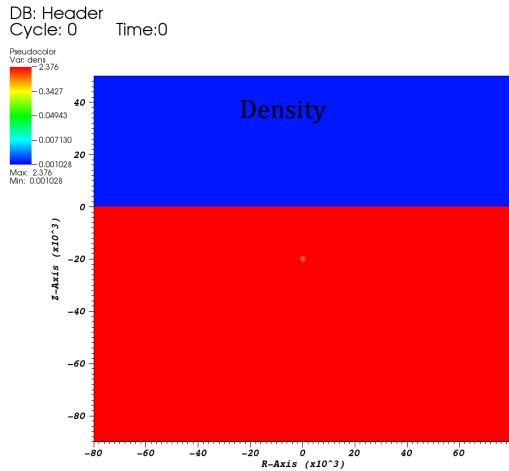 ANFO and with a nuclear surrogate, these pictures do not allow a detailed comparison of these two energy densities. A more definitive comparison is obtained through detailed analysis of the results of the ANFO and nuclear surrogate simulations.

COUPLING FACTOR, OR EQUIVALENT-YIELD FACTOR

The equivalent-yield concept was introduced as a means of quantifying the ground shock produced by a near-surface nuclear explosion of yield, W, in terms of an 'equivalent' nuclear-explosion yield, W_{eq}, of a contained (*i.e.* deeply buried) nuclear explosion "that would produce the same motion and stress field as the near-surface burst"[10,11]. The equivalent-yield-factor, or coupling-factor, C_F, is simply the equivalent yield divided by the total yield of the near-surface explosion, $C_F = W_{eq}/W$.

The most common use for a coupling-factor, C_F, for near-surface nuclear explosions is in describing the lethality-effectiveness of generally downward-propagating ground shocks below the shot point (i.e., related to the effectiveness of the explosion in destroying or severely damaging a buried target structure). According to Drake[11] "the equivalent-yield-factor coupling varies with stress level ranging from nearly one close to the blast, gradually becoming smaller with increasing range". The commonly used 'coupling-curves' for near-surface nuclear explosions are "best-estimates of the equivalent yield-coupling-factor for peak-accelerations, velocities, and stresses in the range of about 1kbar." Such a coupling-factor serves its purpose for comparing weapon effectiveness; however, for this study we desired a comparison tool that was less sensitive to the location where the comparison was made (i.e. avoiding the property of the commonly used Coupling Factor of "gradually becoming smaller with increasing range"). Thus, we sought a comparison method that would be relatively insensitive to the distance at which the 'measurement' point was located relative to the explosive source. We also wanted a comparison method based on signals obtained at near-ground surface locations (i.e., "measurement-points" a meter or two above the ground for air-blast, and a few meters below the ground surface for ground-shock) in the relatively near field (i.e., generally at scaled ranges < 0.5 km/kt$^{1/3}$), in order to be somewhat consistent with potential future forensic analysis of instrumented metropolitan areas, in the event of a clandestine nuclear explosion.

Early in this computational study we looked at the behavior of peak velocity, peak pressure and impulse in the first positive pressure pulse as a function of propagation distance down into the geologic media below the shot point, and confirmed that the commonly used equivalent-yield coupling factor generated for these waves did indeed decrease as the stress level decreased (i.e. it varied with the 'range' or distance selected for the comparison). Use of that coupling factor would require selection of an arbitrary 'nominal' stress level for use in this study (like the 1-kbar stress level used for lethality studies). We sought a comparison approach that could be consistently applied to both air blast and ground-shock waves and would also be relatively insensitive to the specific

ground-surface distance from the shot point where the comparison or 'measurement' is made.

In order to have a robust equivalent-yield approach (i.e., robust with respect to the distance from the shot point where the comparison is made), a reference explosive source is needed for each wave type that exhibits an attenuation vs range behavior (near the ground surface where the air blast and ground shocks would be 'measured') that is similar in character to that exhibited by the near-surface explosions being studied. Our initial selection for the 'reference configuration' for the near-ground-surface air-blast wave was a free-air explosion, and for the near-surface ground wave, the initial reference configuration considered was a deeply buried explosion.

Air-Blast Behavior – Shock waves produced by explosions in air have been the subject of numerous theoretical, numerical and experimental studies [e.g., ref 7]. Very close to a high-energy-density source, the effective sound speed is many tens of kilometers per second and the expansion is extremely rapid. As this 'fireball' expands the rate of decay of the peak shock pressure initially obeys a nearly inverse R^3 power relationship, from an initial pressure of several GPa down to pressures on the order of 10MPa at a scaled range on the order of 50 m/kt$^{1/3}$. Beyond that distance the expanding pressure decay rate undergoes a gradual transition until it becomes a spherically expanding acoustic wave at scaled distances greater than about 500 m/kt$^{1/3}$. The energy in that acoustic sound wave follows an inverse square law with spherical expansion; but the intensity of sound energy is proportional to the square of the sound pressure, so that a linear inverse relation between overpressure and distance results in the distant acoustic regime for air-blasts. Similarly, ground shocks from deeply buried explosions exhibit one characteristic attenuation behavior near the shot point when the geologic medium is undergoing large plastic deformations, often characterized by a nearly straight power-law attenuation curve with distance (in log-log space), with an eventual transition to an elastic wave regime, with a different characteristic power-law attenuation vs range behavior (i.e., again usually exhibiting a nearly straight-line in log-log space).

The air-blast wave from a near surface burst exhibits nearly the same characteristic attenuation behavior as a free-air burst, but with nearly double the yield of the free-air case (because most of what would be have been a downward-traveling air-blast wave is reflected back up into the air by the nearly rigid ground surface). As the HOB increases above the ground surface, this simple reflected wave model breaks down because the reflected wave travels through shocked air, is refracted and develops a Mach-stem at the base of the expanding ground surface air-blast wave. For scaled HOB's below ~20 m/kt$^{1/3}$ the Mach-stem effect nearly disappears at horizontal ranges exceeding 200 m/kt$^{1/3}$ or so. Based on this behavior we decided that the air-blast from a free-air (or high-altitude) burst would be a reasonable reference source for the surface air-blast wave, with the caveat that the nominal or asymptotic coupling-factor would be a value of 2 instead of the customary 1 (or we could simply scale the 'raw' coupling factor by 0.5 to obtain an air-blast coupling-factor that gives a value of approximately 1 for HOB's around 20 m/kt$^{1/3}$).

Near-surface-ground-motion – The simulated attenuation behavior of near-surface ground-shock waves at horizontal ranges of 100 m to 700 m did not show attenuation behavior that mimicked the distance dependent attenuation of deeply buried explosions in

the limestone used for this computational study (primarily because of the effects the free-surface reflection at the air-limestone interface had on the outgoing near-surface ground shock). We did find, however, that near surface ground-shock waves from modestly deep emplacements (e.g. scaled DOB's at or below -30 m/kt$^{1/3}$, or so, which had very little, if any, air-blast wave created) did exhibit near-surface ground-shock wave attenuation behavior (vs distance) that was very similar to that exhibited by waves from more shallowly buried explosions. In addition the downward propagating waves from the ~35 m/kt$^{1/3}$ DOB explosions exhibited stress vs distance behavior that was identical to that calculated for deeply buried explosions. Thus, we used simulations of explosions buried at 30 or 35 m/kt$^{1/3}$ as the 'reference signal' against which near-surface ground shock waves from various emplaced explosions could be compared. Doing this we found that we could compare the peak pressure, or peak velocity, in the first positive ground motion wave at various distances to the same signal from the reference case to obtain a consistent 'coupling-factor' for the near-surface ground motion (relatively far from the event, e.g. at various scaled ranges > 200 m/kt$^{1/3}$). This approach worked adequately for almost all configurations simulated; however, for air-bursts that coupled poorly to the ground, the ground shock wave ended up exhibiting a relatively complex time-history, with the second pulse arriving at the near-air-surface monitoring points having a higher peak pressure or velocity than the first positive pressure pulse. For those few cases we manually examined the time-history behavior at selected locations to obtain the peak-pressure vs. range attenuation curve for that particular emplacement.

Coupling-Factor Calculation – In this computational study selected monitoring-points for recording time-histories of all hydrodynamic variables were located at specified horizontal distances from the shot point in the air, 2 m above the ground surface, and in the ground, 5 m below the ground surface. To obtain the reference 'free-air' baseline values a simulation at HOB = 200 m/kt$^{1/3}$ was used with monitoring points located at selected distances along a radial line (extending up at 45°, to avoid the axis in this 2D axisymmetric simulation, and to avoid any effects of the reflected wave from the ground). The reference case for the ground motion was an explosion placed at a depth DOB = -35 m/kt$^{1/3}$. Separate chemical explosive (ANFO) and nuclear (iron-gas) simulations created separate 'reference' baseline signals for the two types of explosions. The time-traces for each of the reference simulations at each monitoring location were processed to obtain a peak pressure vs distance set of points for each of the four reference cases (e.g. ANFO-Air, ANFO-DOB$_{35m}$, Nuc-Air, Nuc-DOB$_{30m}$).

A few assumptions are made in order to obtain the coupling-factor values. We assume that the reference attenuation curve (e.g., P vs Range) would scale with the well-known yield-to-the-one-third power-scaling rule, (e.g., W$^{1/3}$). We further assume that the local shape of the attenuation curve can be well characterized by a piecewise linear curve in log-log space (i.e., that the reference attenuation curve is nearly like a power-law relation, with a slowly changing exponent, $P_r \sim P_0 R^{-n}$, at least locally). As illustrated in the schematic shown in Figure 9, the reference attenuation curve is used to determine a reference range R_1 where a 1-kt explosion (in the reference configuration) would produce a peak ground shock (or air blast) pressure equal to the measured pressure, P_m ('measured' or monitored at a range, R_m, from the explosion point).
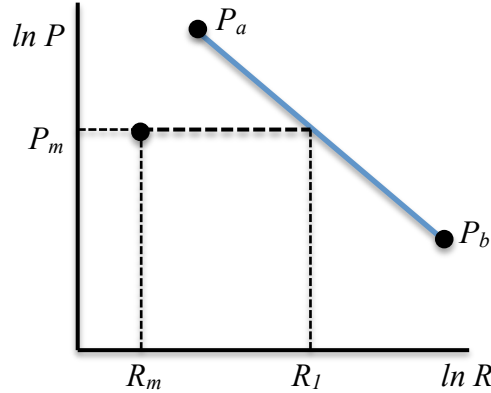
Figure 9. Schematic showing various values used in estimating a value for the coupling factor, C_F, from the reference attenuation curve, represented by the line from P_a to P_b in the image.

The point (R_m, P_m) is the 'measured' point, the range or radius R_1 is the range where the reference explosion would produce a 'peak-pressure' of magnitude P_m. Once the reference range R_1 is obtained, it can be used along with the range, R_m, where the peak pressure, P_m, was measured (or monitored in the simulations) using the familiar $W^{1/3}$ hydrodynamic similarity scaling relation for pressure, or velocity, to determine the equivalent yield, W_{eq} of an explosion in the reference configuration that would produce the measured pressure, P_m, at the measured range, R_m,

$$W_{eq} = \left(\frac{R_m}{R_1}\right)^3.$$

The coupling factor, C_F, is the ratio of the equivalent yield, W_{eq}, to the reference yield $(W_1 = 1 \text{ kt})$, or,

$$C_F = \frac{W_{eq}}{W_1}.$$

The coupling factors shown in the summary curves of Figure 10(a) and 10(b) are the values of $C_{FG} = W_{eq}/W$ for the near-surface ground-shock waves monitored at a depth of 5 m at distances between 100 m and 600 m away from the shot point. The coupling factors for the air-blast waves are half of the value generated by the 'raw' coupling factor calculation using a free-air explosion as the reference curve, $C_{FA} = \frac{1}{2} W_{eq}/W$.

Figures 10(a) and 10(b) show the results of this detailed comparison. The reference curves for the ANFO coupling factor curves are simulations of ANFO explosions (free-air or 35 m DOB) and the coupling factor curves for the Nuclear case are simulations of high-energy-density 'iron-gas' sources with 1-kt of internal energy in 'free-air' or 35 m DOB configurations. These curves do not show any cross-correlation values (i.e., using ANFO simulation results to predict nuclear results, or vice versa). Such cross-correlations could be made using the simulation results of this study; however, no such comparisons were made.
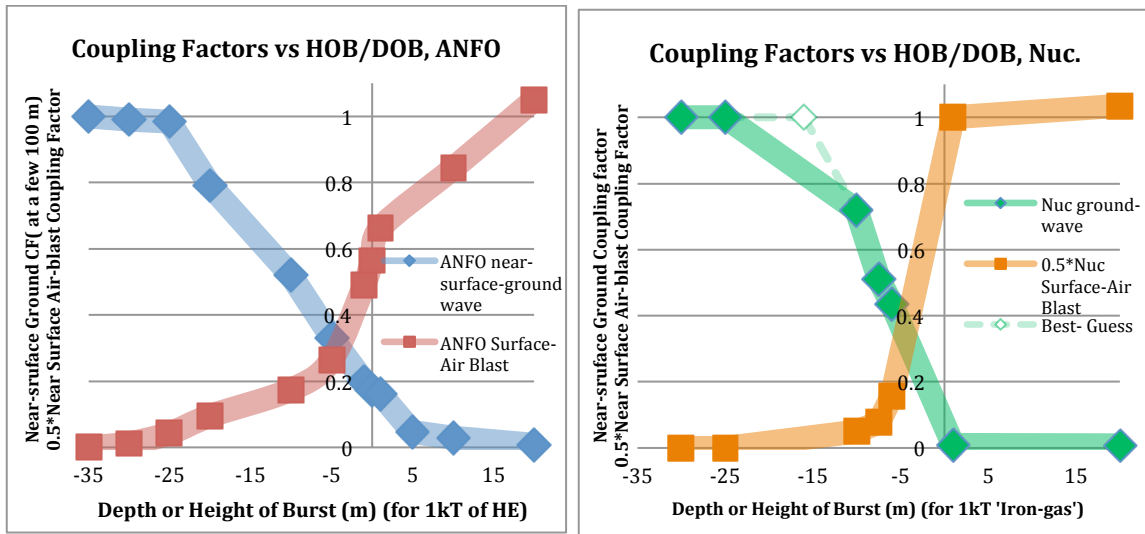
Figure 10 (a) Coupling Factor curves obtained from this computational study for 1-kt ANFO explosive sources at various heights and depths, (b) the same type of coupling-factor curves for simulated nuclear explosive sources at various emplacement heights and depths. The point in (b) labeled 'best guess' is an estimate of what the result might be if a simulation had been run at a depth of burial of 15m with the nuclear simulated source (this case was not in the suite of configurations set up). Based on the similarity of the ground-coupling curve between the ANFO calculations and the nuclear source calculations the point on the dotted curve was estimated. The calculation is now in progress and will be updated when the calculation is complete.

The key items to notice is that the transition of the air blast curve from fully decoupled to fully coupled occurs almost entirely between 5 meters depth of burial to 1 meter height of burst for the simulation of a nuclear device. The transition of the air blast curve from fully decoupled to fully coupled occurs much more gradually for the calculations using ANFO. In fact this transition occurs between 25 meters depth of burial to 15 meters height of burst. The curves showing the energy coupled into ground shock are not as dramatically different with the ANFO curves going from fully decoupled to fully coupled between 5 meters height of burst to 25 meters depth of burial, and the simulated nuclear curves going from fully decoupled to fully coupled between 1 meter height of burst to ~15 meters depth of burial.

COMPARISON WITH OTHER RECENT COUPLING-FACTOR WORK

It may take some additional work to normalize these curves properly. But the trends seem clear based on this series of calculations. A key set of data for comparison with these curves is the work of Rodgers *et al.*[9] based on data from an extensive set of high explosive experiments, the Humble Redwood series (see Figure 11). However it is not a straight-forward comparison as the Humble Redwood explosions were in alluvium while the calculations in this study use limestone equation of state and properties. The physical linear scaling factor between Humble Redwood and our calculations is about 12.

However, the alluvium of the Humble Redwood series has much different constitutive and mechanical properties than the limestone assumed for our calculations.
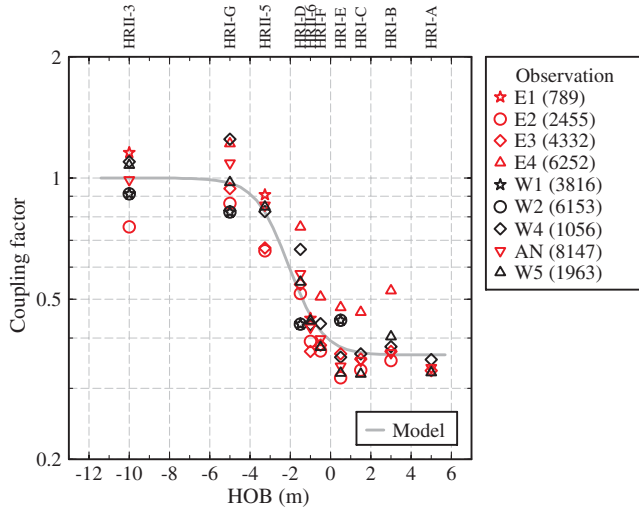

Figure 11. Analysis of the Humble Redwood data, taken from Ref. 3.

As mentioned earlier, this study focused on one representative material (e.g. dry Indiana limestone with modest porosity), and the aim of the study was to determine differences between near-surface HE and nuclear explosions, especially examining differences created during early-time interaction of the explosive with the ground. Similar differences would be expected with other geologic materials; however, determination of the effects of alternative geotechnical material properties and/or layered configurations on signals observed was not part of this investigation. The geologic material in this study was a monolithic block of limestone, with a gradual increase in wave speed with depth caused by the increased lithostatic pressure with depth. This 'geology' is somewhat different than that used in some other recent studies of the effects of explosion on near-surface ground waves. The reader is reminded of this, because at first glance other recent studies of ground coupling from explosions appear to indicate significantly different behavior than is shown for the near-surface ground-ground wave in Figure 10. There are many similarities, but also some important differences between this work and the ground-coupling factor described by Ford et $al.$[3] Ford's ground coupling-factor is fit with a functional form that includes a power-law attenuation with distance (e.g. $\log_{10}(d_s) = \beta_1 + \beta_2 \log_{10}(r_s)$, where d_s is the ground displacement measured near the surface at a distance, r_s away from the explosion, and β_1 and β_2 are empirically determined coefficients). This approach is quite similar to the coupling factor estimation approach utilized in this work; however, the height dependence of this coupling factor in Ford et $al.$'s work differs substantially from the results of this study. They empirically fit a 3-parameter hyperbolic tangent function (a function that produces flat asymptotes at each end of the DOB-HOB spectrum), which is shifted to produce a coupling factor of 1.0 for deeply buried events. When the data and empirical fit of Ford et $al.$ is compared to the coupling factor results obtained in this study, two very significant differences are immediately apparent: 1) the

Ford *et al.* data (for high-explosive tests in dry alluvium) have a much slower variation of coupling-factor for measured near-surface ground displacement than does the peak-pressure coupling factor resulting from simulations in limestone from this computational study; and 2) at scaled heights significantly higher than those in this study the near-surface-displacement coupling factors measured in dry alluvium show a value that asymptotes to a value near 0.35, instead of the near-zero values obtained for peak-pressure coupling-factors for HOB's greater than $5 \, m/kt^{1/3}$, found in this computational study.

The fact that dry alluvium would exhibit a variation of coupling over a wider range of heights/depths is not surprising, since alluvium is a significantly weaker material than the Indiana limestone modeled in this study. Whether changing the material strength in the simulated monolithic material to a value closely resembling that of alluvium would produce as large a difference in height over which the coupling factor varies as is seen in the measurements in alluvium is not known; however the GEODYN code was previously used by a different team at LLNL to simulate the Humble Redwood series of HE tests in alluvium, and was able to fit the measured wave shapes and magnitudes reasonably well.

The higher asymptote (e.g. a coupling factor near 0.35 instead of near zero for scaled HOB's greater than $10 \, m/kt^{1/3}$) requires phenomena other than just a lower strength in the geologic material to explain. The most likely cause of the significant measured near-surface ground-wave signals from bursts that were so high above the dry alluvium surface, is the inherent layering of the dry alluvium in the high-explosive New Mexico tests (e.g., Humble Redwood, Dipole Might, and Divine Buffalo). For example, the alluvium at the Humble Redwood site was modeled (at least for one side of the site) as consisting of 4 distinct layers with the following properties: Layer 1 (the topmost layer) had a sound-speed $c_1 \sim 355m/s$, density, $\rho_1 \sim 1.53g/cc$, porosity, $\varphi_1 \sim 0.42$; Layer 2, $c_2 \sim 600m/s$, $\rho_2 \sim 1.56g/cc$, $\varphi_2 \sim 0.41$, Layer 3, $c_3 \sim 975m/s$, $\rho_3 \sim 1.63g/cc$, $\varphi_3 \sim 0.38$; Layer 4, $c_4 \sim 2000m/s$, $\rho_4 \sim 1.98g/cc$, $\varphi_4 \sim 0.25$. In our limestone simulation study the downward traveling ground shock from airbursts higher than $5 \, m/kt^{1/3}$ had a quite high magnitude, even though the near-surface ground wave traveling horizontally out from the shot point was quite small and produced almost no signal at distances beyond $300 \, m/kt^{1/3}$ or so. Layering (with higher sound-speed and higher density material at lower depths) causes reflections of downward traveling stress waves. At this point we suspect that the high signals seen in the alluvium measurements are very likely the result of reflection/refraction of the downward traveling wave from the explosions off of the denser, higher sound-speed layers below. This is partially confirmed by the fact that previous calculations using layered alluvium models are able to reasonably reproduce the ground motion observed in these experimental studies.

References

[1] K.B. Fournier, C. G. Brown Jr., M. J. May, W. H. Dunlop, S. M. Compton, J. O. Kane, P. B. Mirkarimi, R. L. Guyton, and E. Huffman, "Energy Partitioning, Energy Coupling (EPEC) Experiments at the National Ignition Facility" *Journal of Radiation Effects, Research and Engineering* **30**, 119 (2012).

[2] K. B. Fournier, C. G. Brown Jr., M. J. May, S. Compton, O. R. Walton, J. O. Kane, P. B. Mirkarimi, and W. H. Dunlop, "Final Report on the Energy Partitioning, Energy Coupling Experiments Project at the National Ignition Facility", *LLNL technical report LLNL-TR-644342*.

[3] S. R. Ford, A. J. Rodgers, H. Xu, D. C. Templeton, P. Harben, W. Foxall and R. E. Reinke, "Partitioning of Seismoacoustic Energy and Estimation of Yield and Height-of-Burst/Depth of-Burial for Near-Surface Explosions", *Bulletin of the Seismological Society of America* **104**, April 2014.

[4] I. Lomov, "Simulation of Dense and Dilute Multiphase Compressible Flows with Eulerian-Lagrangian Approach", *LLNL technical report UCRL-PROC-231305*, in Proc. of 6th International Conference on Multiphase Flow, ICMF 2007, Leipzig, Germany, July 9–13, 2007

[5] Y. Kanarska, I. Lomov, L. Glenn, and T. Antoun, *Ann. Nucl. Energy* **36**, 1475 (2009).

[6] I. Lomov, R. Pember, J Greenough, B. Liu, "Patch-Based Adaptive Mesh Refinement for Multimaterial Hydrodynamics", *LLNL technical report UCRL-CONF-2164444*, in Proc. of Joint Russian-American Five-Laboratory Conference on Computational Mathematics, Vienna, June 19–23, 2005.

[7] G. F. Kinney and K. J. Graham, *Explosive Shocks in Air* (Springer-Verlag, 1985).

[8] S. Glasstone and P. J. Dolan, *The Effects of Nuclear Weapons*, 3rd ed. (United States Department of Defense and United States Department of Energy, 1977).

[9] A. J. Rodgers, H. Xu, D. C. Templeton, A. L. Ramirez, V. Chipman, S. R. Ford, D. H. Chambers, "Estimation of Yield and Height-of-Burst for Near-Surface Explosions from Joint Inversion of Air-Blast and Seismic Data" presented at the Fall 2011 American Geophysical Union Meeting, San Francisco, CA, December 5-9, 2011.

[10] H.F. Cooper Jr., "Empirical Studies of Ground Shock and Strong Motions in Rock," R&D Associates, October 1973.

[11] J.L. Drake, S.E. Blouin, and E.B. Smith, "Ground Shock Beneath near Surface Explosions – the DUG Methodology," ARA Report for Contract DNA 001-86-C-0149, DNA-TR (unknown final DNA number), November, 1988